INTERNATIONAL JOURNAL FOR NUMERICAL METHODS IN FLUIDS
Int. J. Numer. Meth. Fluids 2008; **56**:23–35
Published online 16 May 2007 in Wiley InterScience (www.interscience.wiley.com). DOI: 10.1002/fld.1521

Calculation of nonlinear aerodynamic characteristics of a wing using a 3-D panel method

Jeonghyun Cho and Jinsoo Cho*, †

School of Mechanical Engineering, Hanyang University, Seoul 133-791, Republic of Korea

SUMMARY

The nonlinear aerodynamic characteristic of a wing is investigated using the frequency-domain panel method. To calculate the nonlinear aerodynamic characteristics of a three-dimensional wing, the iterative decambering approach is introduced into the frequency-domain panel method. The decambering approach uses the known nonlinear aerodynamic characteristic of airfoil and calculates two-variable decambering function to take into consideration the boundary-layer separation effects for the each section of the wing. The multidimensional Newton iteration is used to account for the coupling between the different sections of wing. The nonlinear aerodynamic analyses for a rectangular wing, a tapered wing, and a wing with the control surface are performed. Present results are given with experiments and other numerical results. Computed results are in good agreement with other data. This method can be used for any wing having different nonlinear aerodynamic characteristics of airfoil. The present method will contribute to the analysis of aircraft in the conceptual design because the present method can predict the nonlinear aerodynamic characteristics of a wing with a few computing resources and significant time. Copyright © 2007 John Wiley & Sons, Ltd.

Received 28 September 2006; Revised 3 April 2007; Accepted 4 April 2007

KEY WORDS: nonlinear aerodynamic characteristics; frequency-domain panel method; iterative decambering approach; Newton iteration; kernel function

1. INTRODUCTION

After the linear aerodynamic method such as Prandtl's lifting-line theory (LLT) to predict the lift and induced drag of wings at small angle of attack was well established, then the LLT became a standard tool for calculating wing aerodynamics. In this method, a lift-curve slope is assumed for the airfoil sections that form the wing. With the success of LLT in the prediction of the

*Correspondence to: Jinsoo Cho, School of Mechanical Engineering, Hanyang University, Seoul 133-791, Republic of Korea.
†E-mail: jscho@hanyang.ac.kr

Contract/grant sponsor: Hanyang University; contract/grant number: HY-2004-I

aerodynamic characteristics of wing at small angle of attack, researchers have attempted to extend this linear prediction method to treat the analysis of wings where nonlinear lift-curve slopes for the airfoil sections can be taken into consideration. The desire to predict nonlinear aerodynamic characteristics of wings using experimental or computational section data for these high angles of attack provided the motivation to researchers. The prediction method such as a 'strip-theory' is used by the need for rapid prediction capabilities for such high angle of attack in the conceptual design phases. However, it is recognized that the flow over a wing at high angle of attack is highly three-dimensional and that a 'strip-theory' approach brings the considerable error. Furthermore, even high-fidelity computational fluid dynamics (CFD) techniques where they can be reliably used for high angle of attack aerodynamic prediction require large computing resources and significant time even for the analysis at a single angle of attack. These CFD techniques need user's desperate efforts such as the time required for generating high-quality grids for each configuration. Thus the research for approximate approaches for stall prediction of wings using the known section airfoil data continues to be of interest. Tani [1] has developed the first successful technique for handling nonlinear section lift-curve slopes in the LLT formulation in 1934. This method worked well up to the beginning of stall and was generalized by the NACA report of Sivell and Neely [2] in 1947. However, this successive-approximation approach appears to fail at high angle of attack where some sections on the wing may have a negative lift-curve slope. Schairer and Sears investigated the possibility of nonunique solutions of Prandtl's lifting-line equation. According to Sears [3], Prandtl's lifting-line equation has nonunique solutions and asymmetric lift distributions for cases when some sections of the wing may have negative lift-curve slope. Piszkin and Levinsky [4] developed a nonlinear lifting line method based partly on the iterative method originally proposed by Tani. The need for a method that could predict adverse wing stalling characteristics such as wing drop provided motivation to them. These characteristics were caused by the occurrence of asymmetric lift distributions on the wing with stalled or partially stalled flow. The Piszkin–Levinsky method has been used until a recent date for aircraft high angle of attack stability analysis. After Levinsky's publication [5], Anderson *et al*. [6] applied a nonlinear LLT to drooped leading-edge wings below and above stall. Tseng and Lan [7] suggested an approach to the use of nonlinear section data. They investigated the effect of boundary-layer separation by iteratively reducing the angle of attack at each section of the wing. The reduction of the angle of attack at any given wing section is determined by the difference between the potential flow solution and the viscous lift coefficient from the nonlinear section lift curve. McCormick [8] also proposed a similar approach to examine the loss in roll damping for a wing near stall. Recently, Mukherjee *et al*. [9] and Mukherjee and Gopalarathnam [10] developed a decambering approach wherein the chordwise camber distribution at each section of the wing was reduced to take the viscous effects into consideration at high angles of attack.

The purpose of the present research is to analyse the nonlinear aerodynamic characteristics of three-dimensional wing using the frequency-domain panel method [11, 12]. The frequency-domain panel method uses the kernel function of an integral equation that relates a known or prescribed upwash distribution to an unknown lift distribution for a finite wing. The method has the advantage that it deals with the pressure differential and induced velocity of interest directly. To predict the nonlinear aerodynamic characteristics of wing at high angles of attack, the iterative decambering scheme suggested by Mukherjee and Gopalarathnam is introduced into the frequency-domain panel method. The present method is verified by showing that it produces results that are in good agreement with experiments or other numerical results.

DOI: 10.1002/fld

2. NUMERICAL METHOD

2.1. Frequency-domain panel method

Consider an initial value problem for linearized compressible flow in which the initial disturbances vanish away from the lifting surfaces. A point on a lifting surface $\mathbf{x}_0$ with unit normal $\mathbf{n}_0$ is assigned a transformed pressure differential $\Delta p = \rho_\infty U_\infty P$. (We will assume that $\mathbf{n}_0$ has no component in the freestream or x direction. The flow has speed U_∞, density ρ_∞, and the Mach number M.) The lifting surface induced a transformed velocity at an arbitrary point $\mathbf{x}$, in an arbitrary direction $\mathbf{n}$, which is given by an integral over the lifting surface:

$$w(\mathbf{x}) = \iint K(\mathbf{x}, \mathbf{x}_0) P(\mathbf{x}_0)\, \mathrm{d}S \tag{1}$$

The kernel is the fundamental solution of the reduced wave equation corresponding to the velocity w induced at $\mathbf{x}$ by a point load applied at $\mathbf{x}_0$. In the standard problem, w is specified on the surface and we solve for the load P. The integral is discretized, for simplicity, by a piecewise constant approximation:

$$[w] = [C][P] \tag{2}$$

where C is the integral of K over each panel, and P is to be thought of as a vector of loads on all panels. The problem then is to develop efficient methods for evaluating the coefficients C, with accuracy consistent with the discretization errors in Equation (2).

The unsteady nonplanar kernel K can be abbreviated as (see Figure 1)

$$K = \overline{K}_p K_0 + D\mathbf{n}_0 \cdot \xi K_{p0} \tag{3}$$

where $\xi = (y - y_0)\mathbf{j} + (z - z_0)\mathbf{k}$. The quantities K_{p0} and K_p are the steady planar and nonplanar kernels, respectively. The factor $\overline{K}_p$ is the ratio of the unsteady to steady planar kernels. The coefficient D is given in terms of derivative of $\overline{K}_p$

$$D = \mathbf{n} \cdot \left(\mathbf{i}\frac{\partial}{\partial X} + \boldsymbol{\xi}\frac{1}{\xi}\frac{\partial}{\partial \xi} \right) \overline{K}_p \tag{4}$$

where $X = x - x_0$. Note that in a steady flow, $\overline{K}_p = 1$ and $D = 0$. The singular point is that $\overline{K}_p$ is a regular function and so can be treated as nearly constant over the quadrilateral panel, while

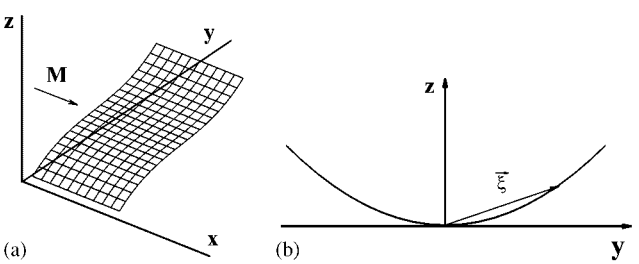

Figure 1. Nonplanar lifting surface: (a) surface and panel geometry and (b) coordinate system.

DOI: 10.1002/fld

its derivatives can be evaluated by finite differences. Therefore, the influence coefficient C is approximated by

$$C = \overline{K}_p C_0 + DC_{p0} \tag{5}$$

where C_0 and C_{p0} are the steady nonplanar and planar influence coefficients, respectively, which can be evaluated analytically. The unsteady factor $\overline{K}_p$ and D are evaluated at only one point on the panel.

Unsteady factor $\overline{K}_p$ depends only on relative axial and radial separations X and ξ, as well as the Mach number and the scaled complex Laplace variables $\overline{s} = s/U$. Since the function is nondimensional, it must depend only on the products $\overline{s}X$ and $\overline{s}\xi$. In the current work, we take it to be

$$\overline{K}_p = \overline{K}_p(sx, sy; M, \Phi) \tag{6}$$

where $sx = |\overline{s}|X$ and $sy = |\overline{s}|\xi$, and Φ is the argument of $\overline{s}$. The range of sx and sy are set by the largest desired magnitude of $\overline{s}$ and the geometry of the body. This range is determined *a priori*, and the function $\overline{K}_p$ is then tabulated on a rectangular grid covering the range, with a grid density, which is somewhat finer than resolution of the panelling that is to be used. Values of $\overline{K}_p$ and its derivatives are then found by interpolation in the table when the influence coefficient matrix is computed. The advantage of this scheme is that the number of kernel evaluations scales with the number of panels, rather than the square of the number of panels as would be the case if the evaluations were done as needed. Furthermore, the table does not need to be reconstructed for any values of $\overline{s}$ with smaller magnitude than that used to define the table. This table is reconstructed only when M, Φ, or the geometry is modified. Further details will be found in References [11, 12].

2.2. *Iterative decambering approach*

The following section has been adapted from References [9, 10]. The decambering for an airfoil is computed using a function of two variables δ_1 and δ_2. These two variables are used because the decambering is determined using the difference between the viscous and the potential-flow results (ΔC_l and ΔC_m). The viscous C_l and C_m of the airfoil can be obtained from experimental or computational data and the corresponding potential flow C_l and C_m are calculated using the frequency-domain panel method:

$$\Delta C_l = (C_l)_{\text{visc}} - (C_l)_{\text{potential}} \quad \text{and} \quad \Delta C_m = (C_m)_{\text{visc}} - (C_m)_{\text{potential}} \tag{7}$$

The values of δ_2 and δ_1 in radians for a given ΔC_l and ΔC_m have been derived from Equations (8) and (9), respectively:

$$\delta_2 = \frac{\Delta C_m}{\frac{1}{4}\sin 2\theta_2 - \frac{1}{2}\sin\theta_2} \tag{8}$$

$$\delta_1 = \frac{\Delta C_l - [2(\pi - \theta_2) + 2\sin\theta_2]\delta_2}{2\pi} \tag{9}$$

$$\theta_2 = \cos^{-1}(1 - 2x_2/c) \tag{10}$$

The lifting surface is divided into several spanwise and chordwise panels. Unlike in the two-dimensional case, changing a δ on one section is likely to have a significant effect on the neighbouring sections of the lifting surface in the three-dimensional case. To take these effects into

DOI: 10.1002/fld

consideration, a $2N$-dimensional Newton iteration is used to calculate the δ_1 and δ_2 at each of the N sections of all the wings. Newton iteration is repeated until the ΔC_l and ΔC_m at these sections close to zero. Further details will be found in References [9, 10].

3. RESULTS AND DISCUSSION

3.1. Two-dimensional results

The convergence history of lift coefficient for a rectangular wing with aspect ratio of 10 at Mach number of 0.1 is shown in Figure 2. As can be easily seen in Figure 2, the lift coefficient converges as the residuals close to zero.

In Figures 3 and 4, to validate the present method for the two-dimensional airfoil, result of the present analysis is compared with experimental result. The nonlinear aerodynamic data of

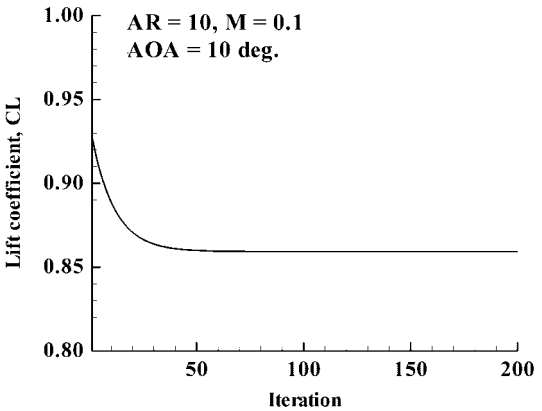

Figure 2. The convergence history of lift coefficient for a rectangular wing.

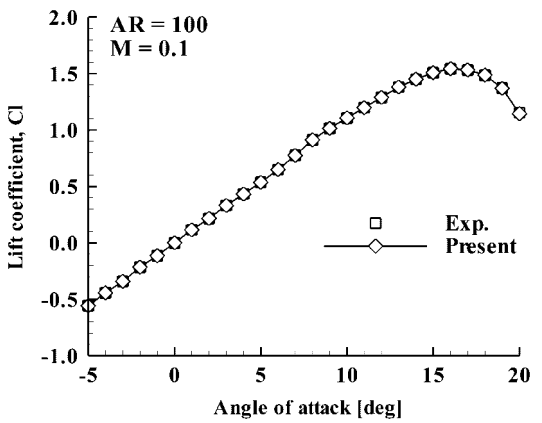

Figure 3. Lift curve of the NACA0012 airfoil.

DOI: 10.1002/fld

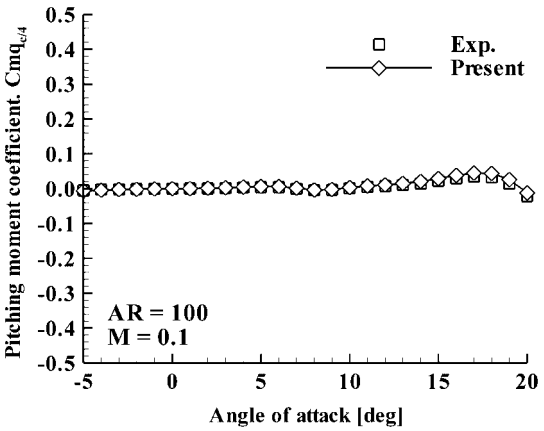

Figure 4. Pitching moment curve of the NACA0012 airfoil.

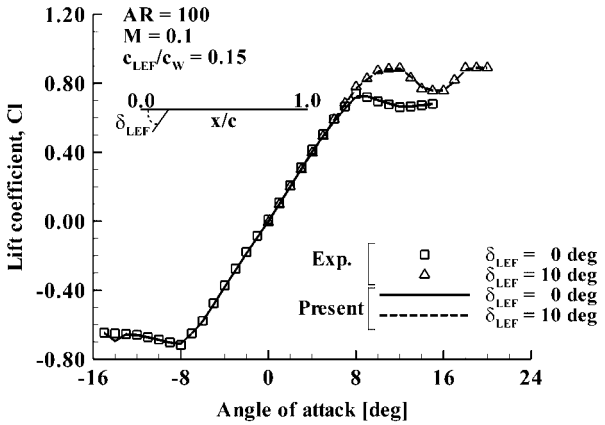

Figure 5. Lift curve of the airfoil with 0.15c plain leading-edge flap.

NACA 0012 is obtained from Reference [13]. To compare the results with those for the case of two-dimensional airfoil, a wing with the aspect ratio of 100 is used. The free-stream Mach number is 0.1. As can be seen in Figures 3 and 4, the present result agrees well with experimental result.

The nonlinear aerodynamic characteristics of two-dimensional airfoil with leading-edge flap are analysed using the present method. The present results are compared with experimental data. The nonlinear aerodynamic data of airfoil with leading-edge flap are obtained from Reference [14]. Wing has the aspect ratio of 100 and the free-stream Mach number is 0.1. The normalized chord ($c_{\mathrm{LEF}}/c_{\mathrm{W}}$) of leading-edge flap is 0.15 and the deflection of leading-edge flap is 10°. The present results coincide with experimental data as can be seen in Figures 5 and 6.

The nonlinear aerodynamic data of two-dimensional airfoil for the analysis of three-dimensional wing with aileron are shown in Figures 7 and 8. The present results are compared with experimental data. The nonlinear aerodynamic data of the airfoil with trailing-edge flap is obtained from

DOI: 10.1002/fld

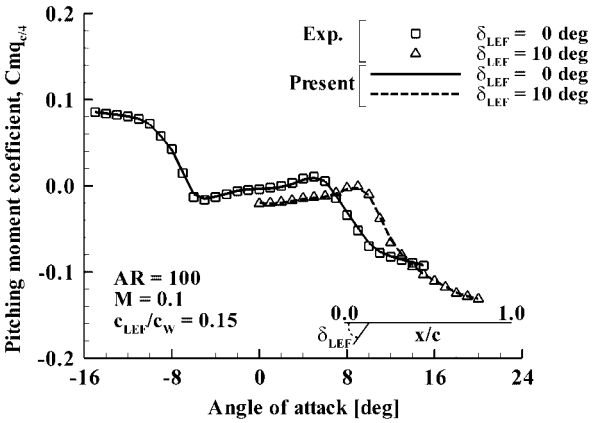

Figure 6. Pitching moment curve of the airfoil with 0.15c plain leading-edge flap.

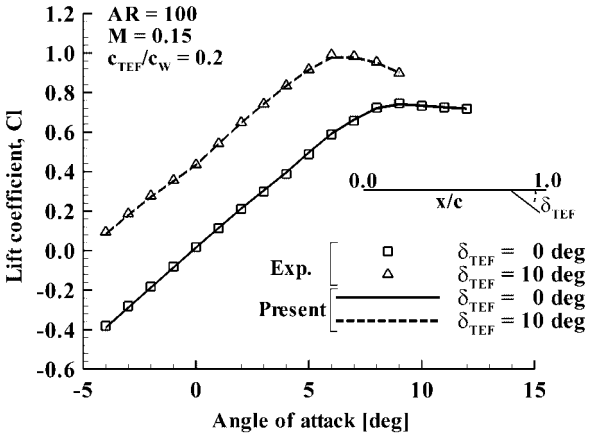

Figure 7. Lift curve of the airfoil with 0.2c sealed plain flap.

Reference [14]. Wing has the aspect ratio of 100 and the free-stream Mach number is 0.15. The normalized chord ($c_{\mathrm{TEF}}/c_{\mathrm{W}}$) of trailing-edge flap is 0.2 and the deflection of trailing-edge flap is 10°. The present results agree well with experimental results as can be seen in Figures 7 and 8.

3.2. Three-dimensional results

The nonlinear aerodynamic characteristics of three-dimensional wing are predicted using the present method. To compare the result with that of Reference [9], which is based on the vortex lattice method, the same assumed nonlinear aerodynamic data are used. These nonlinear aerodynamic data are also similar to those used by Sears and by Levinsky. Wing has the aspect ratio of 10 and the free-stream Mach number is 0.1. Figure 9 shows the three-dimensional lift curve for the rectangular wing. As can be seen in the figure, the present result does agree well with that of

DOI: 10.1002/fld

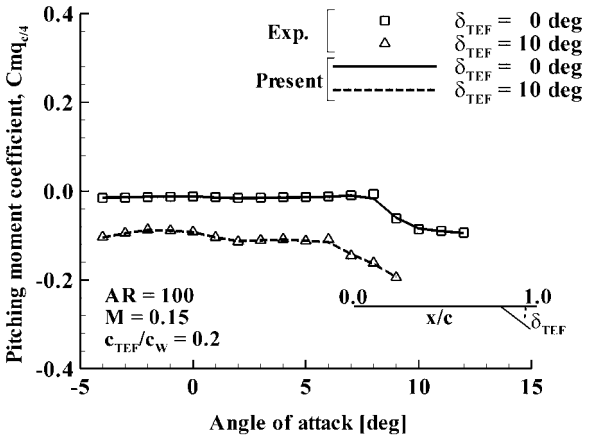

Figure 8. Pitching moment curve of the airfoil with 0.2*c* sealed plain flap.

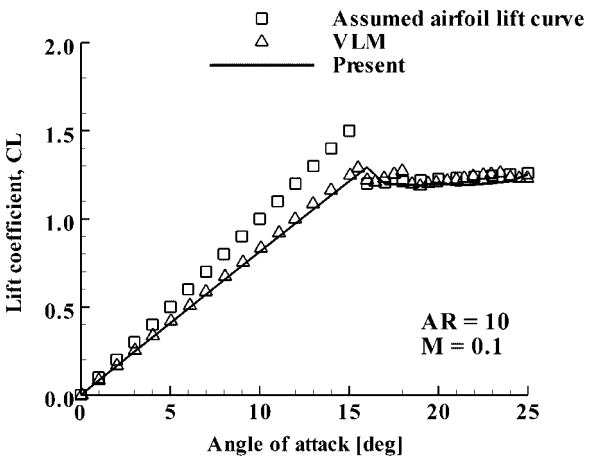

Figure 9. Lift curve of the rectangular wing with aspect ratio of 10.

Reference [9]. In the present method, the multiple intersection scheme [10] is used to eliminate the hysteresis as shown in Reference [9].

The nonlinear aerodynamic characteristics of tapered wing with taper ratio are predicted using the present method. The wing has the aspect ratio of 10 and the sweepback angle of 5° at the leading edge. Free-stream Mach number is 0.1. Figure 10 shows the nonlinear aerodynamic characteristics of tapered wing. It can be seen in the figure that the present results agree well with other numerical results.

The spanwise lift distributions of a rectangular wing with aspect ratio of 10 for the angle of attack are shown in Figure 11. The airfoil has the hypothetical lift curve as shown in Figure 9. The present method predicts the stall of the wing at a slightly higher angle of attack compared to that calculated by the other numerical methods. As the angle of attack is increased beyond 18° the lift

DOI: 10.1002/fld

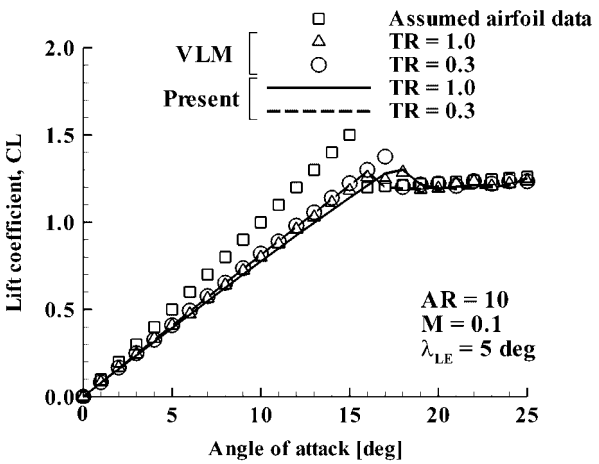

Figure 10. Lift curve of the wing with different taper ratios, each of aspect ratio 10.

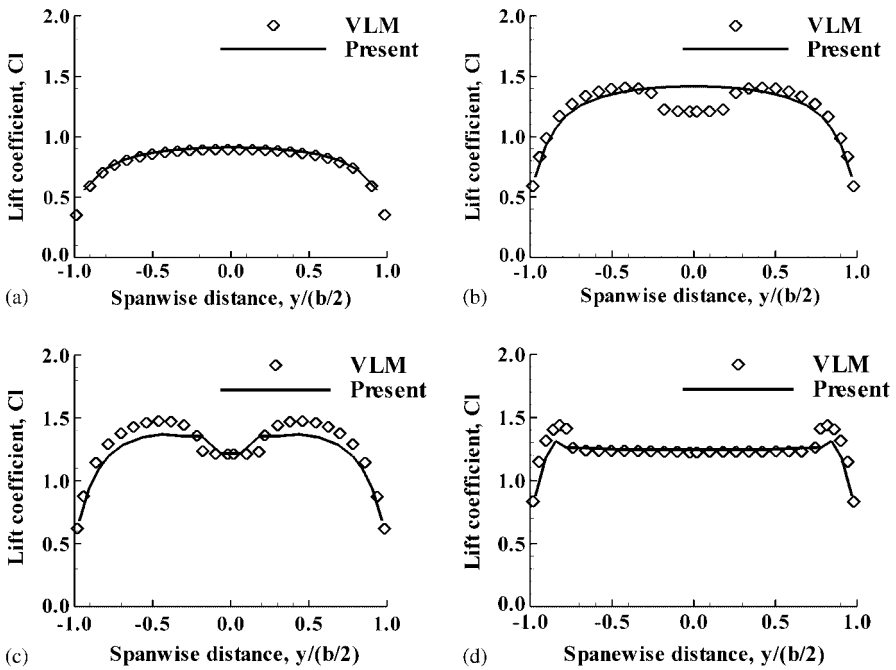

Figure 11. Spanwise lift distributions of the rectangular wing with aspect ratio of 10: (a) AOA = 10°; (b) AOA = 17°; (c) AOA = 18°; and (d) AOA = 24°.

coefficient of the wing is decreased rapidly. Nevertheless, the present results relatively agree well with the other numerical results. In the present method, the multiple intersection scheme [10] is used to eliminate the nonphysical oscillation of the spanwise lift distribution.

DOI: 10.1002/fld

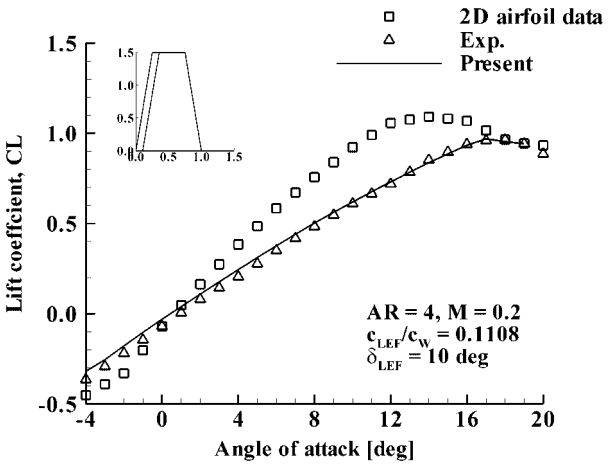

Figure 12. Lift curve of the tapered wing with leading-edge flap.

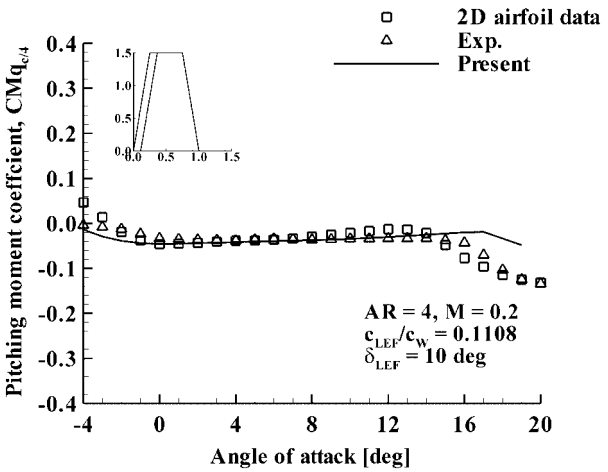

Figure 13. Pitching moment curve of the tapered wing with leading-edge flap.

The nonlinear aerodynamic characteristics of three-dimensional wing with leading-edge flap are predicted using the present method. Results of the present analysis are compared with experimental results. The nonlinear aerodynamic data are obtained from Reference [14]. The wing has the aspect ratio of 4 and the taper ratio of 0.5. The chord of leading-edge flap ($c_{\mathrm{LEF}}/c_{\mathrm{W}}$) normalized with the chord at wing root is 0.1108 and the deflection of leading-edge flap is 10° at the leading edge of the wing. The free-stream Mach number is 0.2. In the experiment, the wing with diamond-shaped airfoil is used. On the other hand, the flat wing without thickness is used in the present calculation because the present method cannot account for the thickness effect of the wing. Besides, the chord of leading-edge flap normalized with the local chord at each section of wing varies from 0.1108 to 0.2217 in the experiment. However, the nonlinear aerodynamic data of the chord of leading-edge flap

DOI: 10.1002/fld

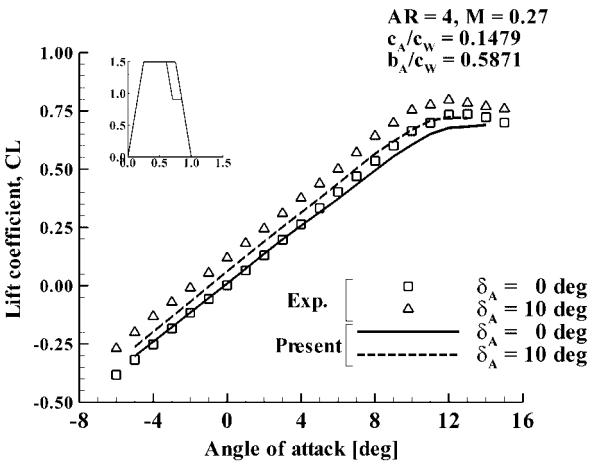

Figure 14. Lift curve of the tapered wing with aileron.

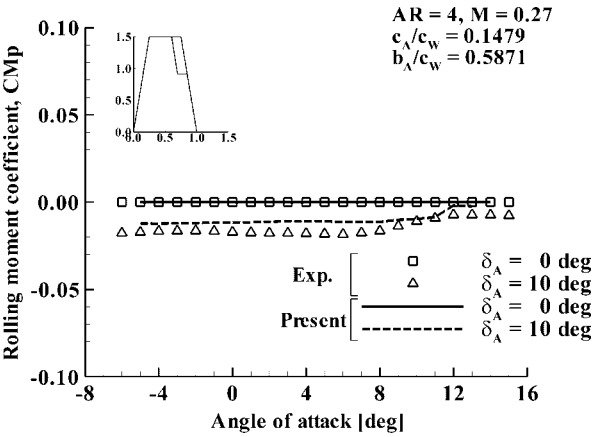

Figure 15. Rolling moment curve of the tapered wing with aileron.

(c_{LEF}/c_W) being 0.15 is used in the present calculation because the proper nonlinear aerodynamic data at each section of the wing were unobtainable. The nonlinear aerodynamic characteristics of tapered wing with leading-edge flap as a function of angle of attack are presented in Figures 12 and 13, respectively. As can be seen in Figures 12 and 13, the present results comparatively agree with experimental results [15].

The nonlinear aerodynamic characteristics of three-dimensional wing with aileron are predicted. The wing has the aspect ratio of 4 and the taper ratio of 0.5. The chord (c_A/c_W) and span (b_A/c_W) of aileron normalized with the chord at wing root are 0.1479 and 0.5871, respectively. The deflection of aileron is 10°. The flat wing without thickness is used, in the same way as for the three-dimensional wing with leading-edge flap. Two different nonlinear aerodynamic data of airfoil are used for the analysis of the three-dimensional wing the aileron. At the wing section with aileron,

DOI: 10.1002/fld

nonlinear aerodynamic data of aileron deflection being 10° is used. On the other hand, nonlinear aerodynamic data of aileron deflection being 0° is used at the wing section without aileron. The nonlinear aerodynamic data are obtained from Reference [14] and are shown in Figures 7 and 8. In the experiment, the chord of aileron (c_A/c_W) normalized with the local chord at each section of wing varies from 0.2126 to 0.2958. However, the nonlinear aerodynamic data of aileron chord (c_A/c_W) being 0.2 and aileron deflection being 10° is used similarly at sections of the wing with aileron because the proper nonlinear aerodynamic data of airfoil at each section of wing with aileron were unobtainable. The nonlinear aerodynamic characteristics of tapered wing with aileron as a function of angle of attack are presented in Figures 14 and 15. As can be seen in the figure, the present results relatively agree well with experiment data [16].

4. CONCLUDING REMARKS

The rapid prediction of the nonlinear aerodynamic characteristics of wing is needed for aircraft stability, control, and simulation purposes. In the present research, the frequency-domain panel method coupled with the iterative decambering approach is used to calculate the nonlinear aerodynamic characteristics of three-dimensional wing. Present method uses the known nonlinear aerodynamic data of airfoil to take into consideration the boundary-layer separation effects for each section of the wing. For the iteration process, a multidimensional Newton iteration was used to account for the effect of the decambering at one section of the wing on the aerodynamic characteristics at all of the other sections of the wing. Results are presented for a rectangular wing, tapered wing, and wing with control surface such as leading-edge flap, trailing-edge flap, or aileron at high angle of attack. As can be seen in the figures, the present results agree well with experiments and other numerical results. The present method does not require large computing resources and significant time to predict the nonlinear aerodynamic characteristics of three-dimensional wing, because the present method uses the known nonlinear aerodynamic data of airfoil. Therefore, the present method will be useful for the analysis of aircraft in the conceptual design phase.

ACKNOWLEDGEMENT

This work was supported by the research fund of Hanyang University (HY-2004-I).

REFERENCES

1. Tani I. A simple method of calculating the induced velocity of a monoplane wing. *Report No. 111*, Aeronautical Research Institute, Tokyo Imperial University, 1934.
2. Sivell JC, Neely RH. Method for calculating wing characteristics by lifting-line theory using nonlinear section lift data. *NACA TN-1269*, 1947.
3. Sears WR. Some recent developments in airfoil theory. *Journal of the Aeronautical Sciences* 1956; **23**:490–499.
4. Piszkin ST, Levinsky ES. Nonlinear lifting line theory for predicting stalling instabilities on wings of moderate aspect ratio. *CASD NSC-76-001*, 1976.
5. Levinsky ES. Theory of wing span loading instabilities near stall. *AGARD CP-204*, 1976.
6. Anderson JD, Corda S, Van Wie DM. Numerical lifting line theory applied to drooped leading-edge wings below and above stall. *Journal of Aircraft* 1980; **17**(2):898–904.
7. Tseng JB, Lan CE. Calculation of aerodynamic characteristics of airplane configurations at high angles of attack. *NASA CR-4182*, 1988.

DOI: 10.1002/fld

8. McCormick BW. An iterative non-linear lifting line model for wings with unsymmetrical stall. *SAE Transactions Paper No. 891020*, 1989.
9. Mukherjee R, Gopalarathnam A, Kim SW. An iterative decambering approach for post-stall prediction of wing characteristics using known section data. *AIAA 2003-1097*, 2003.
10. Mukherjee R, Gopalarathnam A. Poststall prediction of multiple-lifting-surface configurations using a decambering Approach. *Journal of Aircraft* 2006; **43**(3):660–668.
11. Cho J, Williams MH. S-plane aerodynamics of nonplanar lifting surfaces. *Journal of Aircraft* 1993; **30**(4):433–438.
12. Cho JH, Han CH, Cho LS, Cho JS. Steady/unsteady aerodynamic analysis of wings at subsonic, sonic, and supersonic Mach numbers using a 3D panel method. *International Journal for Numerical Method in Fluids* 2003; **42**:1073–1086.
13. Abbott IH, Von Doenhoff AE. *Theory of Wing Sections*. Dover: New York, 1959; 452–499.
14. Cahill JF, Underwood WJ, Nuber RJ, Chessman GA. Aerodynamic forces and loadings on symmetrical circular-arc airfoils with plain leading-edge and plain trailing-edge flaps. *NACA Report 1146*, 1947.
15. Johnson BH, Reed VD. Investigation of a thin wing of aspect ratio 4 in the AMES 12-foot pressure wind tunnel. IV: The effect of a constant-chord leading-edge flap at high subsonic speeds. *NACA RM-A8K19*, 1949.
16. Johnson BH, Demele FA. Investigation of a thin wing of aspect ratio 4 in the AMES 12-foot pressure wind tunnel. III: Effectiveness of a constant-chord aileron. *NACA RM-A8I17*, 1948.

DOI: 10.1002/fld